Chapter 2
Controlling the Conductivity in Oxide Semiconductors

A. Janotti, J.B. Varley, J.L. Lyons, and C.G. Van de Walle

2.1 Introduction

Oxide semiconductors occur in a variety of crystal structures and exhibit diverse electronic and optical properties. Controlling the electrical conductivity in oxide thin films and nanostructures is an important step toward their application in electronics and optoelectronics. Here we discuss the results of first-principles studies of the effects of native point defects and impurities on the electronic properties of semiconducting oxides such as ZnO, SnO_2, and TiO_2. We address the possible causes of the often observed unintentional *n*-type conductivity in these oxides and the prospects of achieving *p*-type conductivity. In the case of ZnO and SnO_2, it is found that the unintentional conductivity is not due to oxygen vacancies or cation interstitials, but rather to the incorporation of donor impurities, with hydrogen being a likely candidate. Although the calculations were aimed at understanding the behavior of defects and impurities in bulk single crystals, the main results and conclusions are expected to be valid for thin films and nanostructures.

ZnO, SnO_2, and TiO_2 are wide-band-gap materials and can be made highly conductive [1–8]. Yet the control of conductivity poses serious challenges and constitutes an important step toward the development of electronic devices based on oxide thin films or nanostructures. It has long been thought that intrinsic defects such as oxygen vacancies are responsible for the observed *n*-type conductivity, largely based on experiments in which the conductivity is measured as a function of the oxygen content in the annealing environment [9–15]. Still the identification

A. Janotti (✉) • J.L. Lyons • C.G. Van de Walle
Materials Department, University of California, Santa Barbara, CA, USA
e-mail: janotti@engineering.ucsb.edu

J.B. Varley
Materials Department, University of California, Santa Barbara, CA, USA

Department of Physics, University of California, Santa Barbara, CA, USA

J. Wu et al. (eds.), *Functional Metal Oxide Nanostructures*, Springer Series in Materials Science 149, DOI 10.1007/978-1-4419-9931-3_2,

of oxygen vacancies has remained quite elusive, and recent efforts to enhance the performance of these oxides have highlighted the fact that the causes and mechanisms of conduction are poorly understood. First-principles calculations for ZnO and SnO_2 have casted severe doubts on the hypothesis that oxygen vacancies are sources of conductivity. The results indicate that oxygen vacancies are deep rather than shallow donors and cannot cause conductivity [16–19].

Recent studies indicate that unintentional impurities are most likely the source of the observed unintentional conductivity in oxides [4, 5, 19–26]. Most growth techniques introduce impurities through the sources or as contaminants; even in ultrahigh vacuum, impurities such as hydrogen are present at high enough levels to incorporate in sizable concentrations in materials in which their solubility is high [22]. Hydrogen is indeed a particularly insidious impurity in this respect, since it is notoriously difficult to detect experimentally.

Based on first-principles calculations it has been suggested that interstitial hydrogen is a plausible cause of unintentional doping in ZnO [20–22], a proposal now confirmed by numerous experimental studies [27–31]. Later, it has been proposed that two forms of hydrogen can act as electrically active impurities: interstitial hydrogen, which prefers to attach to an oxygen host atom and diffuses easily, and substitutional hydrogen on an oxygen site, which is more stable and can alternatively be regarded as a complex consisting of hydrogen and an oxygen vacancy [23]. Both these species were predicted to act as shallow donors in ZnO [23] and SnO_2 [19, 24]. These predictions have been recently confirmed by experiments [32, 33].

In Sect. 2.2, the formalism for calculating defect formation energies and the computational approach are described; Sect. 2.3 addresses the electronic properties of native defects and impurities in ZnO, SnO_2 and TiO_2, and Sect. 2.4 concludes the paper.

2.2 Formalism and Computational Approach

The formation energy is a key quantity in the description of the electronic structure and stability of point defects and impurities in solids. Defects that occur in low concentrations have a small or negligible impact on conductivity; only those whose concentration exceeds a threshold will have observable effects. The concentration is determined by the formation energy through the expression

$$c = N_{\text{sites}} \exp(-E^{\text{f}}/kT), \tag{2.1}$$

where E^{f} is the formation energy, N_{sites} is the number of sites on which the defect can be incorporated, k is the Boltzmann constant, and T is the temperature. To illustrate the definition of the formation energy for a point defect [34–36], we take the specific example of an oxygen vacancy in a 2+ charge state in ZnO:

$$E^{\text{f}}(V_{\text{O}}^{2+}) = E_{\text{tot}}(V_{\text{O}}^{2+}) - E_{\text{tot}}(\text{ZnO}) + \mu_{\text{O}} + 2E_{\text{F}}, \tag{2.2}$$

where $E_{\mathrm{tot}}(V_{\mathrm{O}}^{q})$ is the total energy of the supercell containing the defect, and $E_{\mathrm{tot}}(\mathrm{ZnO})$ is the total energy of the ZnO perfect crystal in the same supercell. The Fermi energy E_{F} is the energy of the reservoir in the solid, with which electrons are exchanged. The oxygen atom that is removed is placed in a reservoir with energy μ_{O}, i.e., the oxygen chemical potential. We note that μ_{O} is a variable in the formalism, corresponding to notion that ZnO can be grown under conditions that vary from the oxygen-rich to the oxygen-poor limit. The oxygen chemical potential μ_{O} is subject to an upper bound equal to the energy per atom of an O_2 molecule. The sum of μ_{O} and μ_{Zn} corresponds to the energy of ZnO, which is essentially the stability condition of ZnO. An upper bound on μ_{Zn}, set by the energy per atom of bulk Zn, therefore leads to a lower bound on μ_{O}. Therefore, the range over which the chemical potentials can vary is given by the enthalpy of formation of ZnO (exp.: −3.60 eV [37]).

Defects are usually electrically active, occurring in charge states other than neutral. For each position of the Fermi level, one particular charge state has the lowest energy. The Fermi-level positions at which the lowest energy charge state changes are called *transition levels*. Once the formation energies are known, the transition levels immediately follow by taking energy differences:

$$\varepsilon(q/q') = [E^{\mathrm{f}}(D^{q}; E_{\mathrm{F}} = 0) - E^{\mathrm{f}}(D^{q'}; E_{\mathrm{F}} = 0)]/(q' - q), \tag{2.3}$$

where $E^{\mathrm{f}}(D^{q}; E_{\mathrm{F}} = 0)$ is the formation energy of the defect D in the charge state q when the Fermi level is at the valence-band maximum ($E_{\mathrm{F}} = 0$). When atomic relaxations are fully included in the calculation of the formation energies for both charge states, a thermodynamic transition level is obtained. The experimental significance of this level is that for Fermi-level positions below $\varepsilon(q/q')$ charge state q is stable, while for Fermi-level positions above $\varepsilon(q/q')$, charge state q' is stable. The transition levels should not be confused with the single-particle Kohn-Sham states that result from band-structure calculations for a single charge state. We also note that in optical experiments (luminescence or absorption) the final state may not be completely relaxed, leading to different values for optical levels [35].

Formation energies, such as in (2.2), can be explicitly calculated based on density functional theory (DFT) [38] calculations. DFT calculations have traditionally used the local density approximation (LDA) [39] or generalized gradient approximation (GGA) [40, 41]. The use of DFT-LDA/GGA implies that the band gap is not properly described, and states within the band gap will therefore be affected as well. If these states are occupied with electrons, the formation energy of the defect will also reflect these errors. Several approaches have been developed to overcome these problems: (1) the LDA + U approach [42], which was used to correct the semicore *d* states in ZnO, thus providing a partial correction to the band gap; in conjunction with LDA, the LDA + U results were used to correct defect formation energies and transition levels in ZnO [16–18]. (2) The screened hybrid functional of Heyd, Scuseria, and Ernzerhof (HSE) [43], which is based on the

inclusion of a small fraction of nonlocal exchange in the Hamiltonian within a sphere of a certain radius, thus describes metals and insulators on the same footing; this is important since it allows for the computation of formation energies that take metals as limiting phases in the evaluation of chemical potentials [26, 44]. (3) The Green's-function-based quasiparticle *GW* method [45, 46], which combined with LDA allowed for precise calculations of defect formation energies and transition levels, as illustrated with the case of the self-interstitial in Si [47]. The calculations discussed in this chapter are based on the DFT within the LDA/LDA + U approach, or the screened hybrid functional (HSE). These calculations made use of projected augmented wave potentials [48, 49] to separate valence from core electrons, as implemented in the VASP code [50, 51].

2.3 Results and Discussion

2.3.1 ZnO

Zinc oxide has a direct band gap of 3.4 eV, an exciton binding energy of 60 meV, and is available as large single crystals [1–5]. As such, ZnO has been considered a promising material for light emitting diodes and laser diodes that operate in the blue-UV spectral region, and for high-power, high-frequency, or thin-film transistors. It has also been demonstrated that ZnO can be made in nanostructures with a variety of morphologies such as wires, helices, belts, and springs which can be useful in gas sensors, transducers, and actuators at the nanoscale [52]. However, the development of ZnO for these various applications has been hindered by a lack of understanding and difficulties in controlling the electrical conductivity [1–5]. ZnO in bulk and thin-film forms is almost always *n*-type [2, 53], the cause of which has been hotly debated. In addition, many reports on *p*-type ZnO have appeared in the literature [54–60], but reliability and reproducibility are still questionable.

The observed *n*-type conductivity in "undoped" ZnO has long been attributed to the presence of native point defects such as oxygen vacancies or zinc interstitials [2, 9–11]. However, the identification of such defects in as-grown (as opposed to irradiated) material has been rather vague, and the evidence of their relation to the observed conductivity has always been indirect, e.g., based on the variation of conductivity with O_2 partial pressure in the annealing environment. On the contrary, first-principles calculations indicate that neither O vacancies nor Zn interstitials can explain the observed *n*-type conductivity in ZnO [16–18]. Recent experiments on high-quality bulk single crystals indeed support these results [61, 62].

The calculated formation energy as a function of the Fermi-level position for native donor defects in ZnO, under O-poor conditions, is shown in Fig. 2.1. These calculations were based on a combination of LDA and LDA + U as described in [17, 18]. The results indicate that oxygen vacancy is a deep donor with a transition

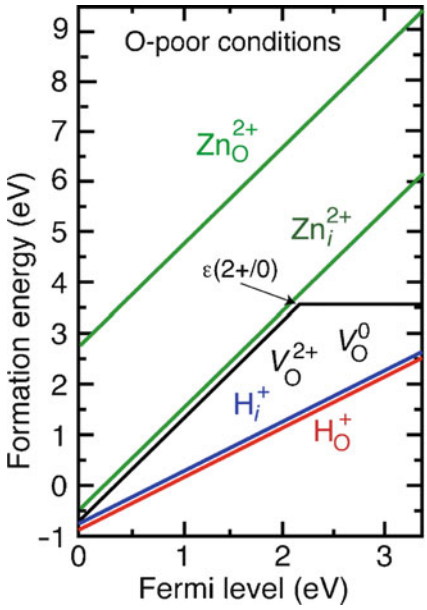

Fig. 2.1 Formation energy as a function of Fermi-level position for donor centers in ZnO: substitutional hydrogen H_O, interstitial hydrogen H_i, oxygen vacancy V_O, zinc interstitial Zn_i, and zinc antisite Zn_O. These were calculated according to the LDA/LDA + U method as described in [18]. Only the results for oxygen-poor conditions are shown. The zero of Fermi level corresponds to the valence-band maximum. The *slope* of the line segments indicates the charge state. The kink in the formation-energy curve of V_O at $E_F = 2.4$ eV indicates the $\varepsilon(+2/0)$ transition level

level $\varepsilon(2+/0)$ about 1 eV below the conduction band. Therefore, V_O is stable in the neutral charge state in *n*-type ZnO and, thus, cannot explain the observed *n*-type conductivity. The ionization energy of ∼1 eV indicates that V_O will not be ionized even at temperatures well above room temperature. The zinc interstitial is a shallow donor, but it is not thermally stable. It has high formation energy in *n*-type ZnO and migrates with an energy barrier of only 0.6 eV [18], i.e., Zn interstitials are mobile even below room temperature. Zinc antisites (Zn_O) are also shallow donors, stable in the 2+ charge state for Fermi-level positions near the conduction band. The large off-site displacement of the Zn atom indicates that Zn_O^{2+} is actually a complex of V_O^0 and Zn_i^{2+}. The high formation energy in *n*-type ZnO indicates that Zn_O^{2+} is unlikely to play a role in the observed unintentional conductivity in as-grown or annealed materials, unless Zn_O^{2+} is created by nonequilibrium processes such as irradiation. Similar results and conclusions based on more sophisticated and computationally demanding hybrid functional methods have been published more recently [63].

Having established that native defects cannot explain the observed unintentional *n*-type conductivity in ZnO, one has to consider the role of impurities that are most likely to be present in different growth environments and act as donors. One such impurity is hydrogen. First-principles calculations have shown that interstitial hydrogen behaves as a shallow donor in ZnO [20, 21]. This is somewhat counterintuitive because hydrogen typically acts as a passivating agent in semiconductors, reducing the electrical conductivity rather than being a source of doping. The theoretical prediction was quickly confirmed in numerous experiments (summarized in [4]).

Nevertheless, interstitial hydrogen is highly mobile [64, 65] and thus can be removed from ZnO by annealing at relatively modest temperatures (~150°C). There are clear experimental indications, however, that hydrogen also exists as a more thermally stable donor that persists upon annealing [29, 66] at temperatures up to ~500°C. Based on first-principles calculations it has been proposed that this additional hydrogen-related donor species consists of a hydrogen atom occupying a substitutional oxygen site [23]. The substitutional hydrogen species is more stable than interstitial hydrogen in ZnO, with a diffusion barrier consistent with the observed reduction in hydrogen activity above ~500°C [29, 66].

The calculated formation energies of interstitial hydrogen H_i and substitutional hydrogen H_O are also shown in Fig. 2.1. Interstitial hydrogen strongly bonds to oxygen, by breaking a Zn–O bond. It can occupy different positions in the ZnO lattice: bond-center and antibonding sites next to oxygen, parallel to the *c*-axis or forming an angle of about 112° with the *c*-axis. In all these configurations, interstitial hydrogen results in effective-mass shallow donor levels, and has similar formation energies, within less than 0.2 eV. We find that the bond-center configuration with an O–H distance of 1.05 Å gives the lowest formation energy. Substitutional hydrogen H_O, on the other hand, bonds equally to all four nearest-neighbor zinc atoms in a multicenter bond configuration and also results in an effective-mass shallow donor. Its formation energy is only ~0.1 eV higher than that of interstitial hydrogen in oxygen-poor conditions. The electronic structure and bonding properties of H_O were discussed in [23]. The formation energy, and hence the solubility of substitutional hydrogen, is consistent with observed concentrations; furthermore, because it replaces oxygen, hydrogen can also explain the observed dependence of unintentional *n*-type conductivity on the oxygen partial pressure in the growth or annealing environments [23].

It has been recently pointed out that other impurities such as Al, Ga, and Si are also present in as-grown ZnO single crystals and act as donors [4]. Al and Ga substitute for Zn and act as shallow donors [67, 68], but are not observed in high enough concentrations to explain the unintentional *n*-type conductivity in bulk single crystals. On the other hand, Si is a double donor when substituting on Zn site [26] and has been found in concentrations that are compatible with free electron concentrations in ZnO single crystals grown by different techniques [25].

Note that controlling the *n*-type conductivity is a necessary step toward achieving the so-desired *p*-type conductivity in ZnO. Despite many reports in the literature, reliable *p*-type doping of ZnO remains difficult. Low solubility of *p*-type dopants and the compensation by abundant donor defects and impurities are often raised as the main issues. Known acceptor impurities include group-I elements Li, Na, K, Cu, and Ag, and group-V elements N, P, and As. However, many of these form deep acceptors and do not result in *p*-type conduction at room temperature. Even N, which has been regarded as the most promising *p*-type dopant in ZnO, has recently been shown to act as a deep acceptor with ionization energy over 1 eV. Calculated results for N-related absorption energy are in good agreement with experimental observations [26].

As an alternative route, it has been proposed that *p*-type conductivity can be achieved by the selective incorporation of interstitial fluorine impurities in ZnO [69]. The F interstitial would complete its octet by extracting an electron from the valence-band maximum. The resulting hole would be bounded to the F impurity in an effective-mass state, as a typical shallow acceptor. It is anticipated that technical difficulties may arise in attempting to selectively introduce interstitial F as majority defects.

2.3.2 SnO_2

Tin dioxide crystallizes in the rutile structure and has a direct band gap of 3.6 eV [12]. The ease of making it *n*-type, its highly dispersive conduction band (small effective mass), and the large energy difference between the conduction-band minimum and the next higher conduction band at Γ contribute to SnO_2 supporting high carrier concentrations while still maintaining a high degree of optical transparency [12]. The fabrication of SnO_2 nanowires and nanobelts has been reported, and gas sensors based on these nanostructures have been demonstrated [70, 71]. These applications crucially depend on the transport of electrons and the control of conductivity. As in ZnO, an unintentional *n*-type conductivity in SnO_2 is likely caused by impurities.

SnO_2 can be doped *n*-type by adding impurities such as Sb or F, which incorporate on Sn and O sites, respectively [12]. In addition, it has been widely believed that oxygen vacancies are also a source of *n*-type conductivity. In analogy to ZnO, the evidence for oxygen vacancies has been based on measurements of conductivity as a function of the oxygen partial pressure in annealing experiments: increasing the oxygen partial pressure leads to lower conductivities [12, 72–75]. However, the attribution of conductivity to oxygen vacancies is not supported by recent first-principles calculations [19, 24].

In Fig. 2.2 we show the calculated formation energies of donor native point defects in SnO_2. These results were obtained from a combination of LDA and LDA + U calculations as described in [19]. As shown in Fig. 2.2, oxygen vacancy is a deep donor, occurring in the neutral charge state if the Fermi level is positioned near the conduction-band minimum. It has also been concluded that Sn interstitials and Sn antisites are unlikely sources of conductivity due to their high formation energies. Therefore, the unintentional *n*-type conductivity is probably caused by the presence of impurities. As shown in Fig. 2.2, it is found that hydrogen in either the interstitial form or substituting for oxygen has also been predicted to act as a shallow donor in SnO_2 [19, 24].

Reports on *p*-type SnO_2 have been scarce. It has been proposed that Ga or In substituting on Sn site would result in shallow acceptors. We anticipate that

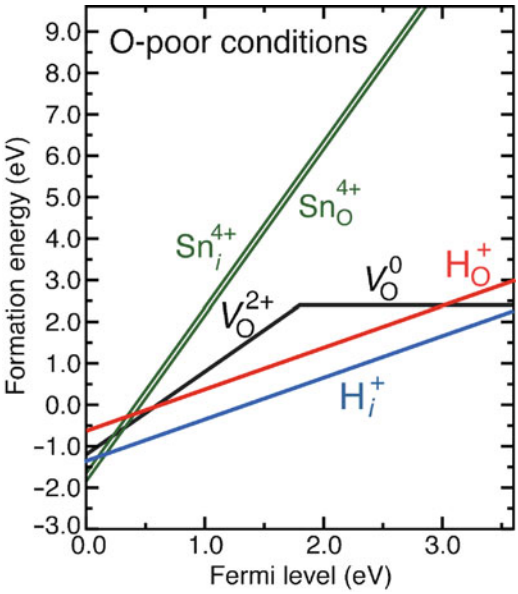

Fig. 2.2 Formation energy as a function of Fermi-level position for donor-type centers in SnO_2: oxygen vacancy V_O, tin interstitial Sn_i, tin antisite Sn_O, hydrogen interstitial H_i, and substitutional hydrogen H_O. These results were obtained using the LDA/LDA + U approach [19]. The zero of Fermi level corresponds to the valence-band maximum. For Fermi-level positions near the conduction band V_O is stable in the neutral charge state whereas Sn_i and Sn_O are stable in the 4+ charge state

difficulties in making SnO_2 *p*-type may arise due to the formation of small hole polarons. The valence band of SnO_2 is quite flat, and instabilities of the O lattice atoms near the impurities may favor the formation of bound hole polarons.

2.3.3 TiO_2

Titania is most stable in the rutile crystal structure and has a band gap of 3.1 eV [37]. The upper part of the valence band is composed of O 2*p* states, and the lower part of the conduction band of Ti 3*d* states [44]. TiO_2 can be made *n*-type by the incorporation of shallow donor impurities (e.g., Nb, F, and H) and by annealing in reducing environments [8, 14]. Because its conductivity varies with O_2 partial pressure, it is often argued that oxygen vacancies and/or titanium interstitials are sources of conductivity in TiO_2 [8, 14].

In Fig. 2.3 we show the calculated formation energies for oxygen vacancies in TiO_2, based on HSE hybrid functional calculations [44]. It was concluded that oxygen vacancies are shallow donors, with V_O^+ and V_O^0 higher in energy than V_O^{2+} for any value of the Fermi level within the band gap [44]. The formation energy of V_O^{2+} in the extreme oxygen-poor limit is relatively low even when the Fermi level is positioned near the conduction-band minimum. This might lead to the conclusion that oxygen vacancies are the cause of conductivity in vacuum-annealed TiO_2. However, care should be taken, since the extreme oxygen-poor limit corresponds to oxygen partial pressures that are not experimentally accessible. We also need to keep in mind that impurities that act as shallow donors, such as hydrogen, also likely contribute to the observed conductivity [76].

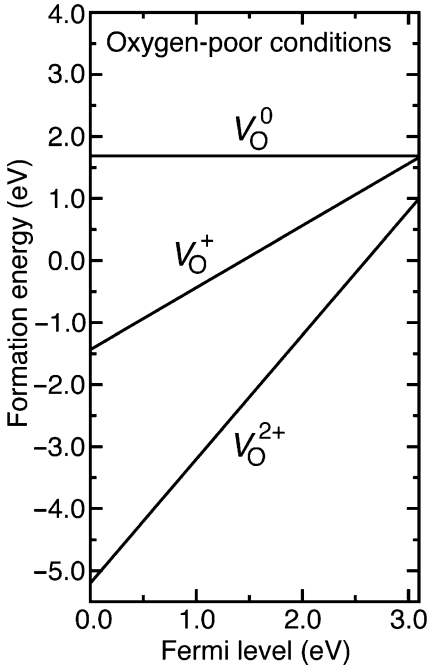

Fig. 2.3 Formation energy as a function of Fermi-level position for the oxygen vacancy V_O in TiO_2. Only the results for the O-poor limit are shown. These were obtained using the HSE hybrid functional. The zero of Fermi level corresponds to the valence-band maximum. V_O^{2+} is lower in energy than V_O^+ and V_O^0 even for the Fermi level positioned at the conduction-band minimum

2.4 Concluding Remarks

We have discussed the causes of conductivity in ZnO, SnO_2, and TiO_2, which are representatives of a large family of wide-band-gap oxide semiconductors. First-principles computational studies indicate that the conventional wisdom of assigning the cause of unintentional conductivity in these materials to the presence of native point defects, such as oxygen vacancies, must be reviewed. In particular it is shown that oxygen vacancies in ZnO and SnO_2 cannot explain the observed conductivity because they are deep donors. Therefore, the widespread view that oxygen vacancies are correlated with conductivity or are easily created during growth or annealing in oxygen-poor, reducing environments must be seriously reconsidered. In addition, first-principles calculations reveal that other native point defects, e.g., cation interstitials, are also unlikely sources of conductivity since they are not thermally stable.

Instead, it is argued that unintentional *n*-type conductivity in oxide semiconductors is more likely caused by the unintentional incorporation of impurities, hydrogen being a prime candidate. Hydrogen is an ubiquitous impurity, being a fast diffuser as an interstitial impurity and also capable of assuming substitutional positions. In both forms, interstitial and substitutional, hydrogen has been predicted to act as shallow donor in these materials. These findings are quite unexpected and have important technological implications, and have been confirmed in the case of ZnO. More experiments need to be performed in the case of SnO_2 and TiO_2.

We also would like to emphasize that hydrogen is by no means the *only* shallow donor impurity that can be unintentionally incorporated; many other impurities may act as shallow donors, such as those on the right (*n*-type) side (in the Periodic Table of Elements) of the element being substituted, although it is quite unlikely that they are present in all growth or annealing environments. Yet hydrogen is present in almost all growth environments, generally hard to detect experimentally, and is not usually considered as a potential donor. Therefore, special attention should be devoted to its potential effects on the electronic properties of oxide semiconductors.

Acknowledgments This work was supported by the NSF MRSEC Program under award No. DMR05-20415 and by Saint-Gobain Research. Collaborations with M. D. McCluskey, M. Scheffler, A. K. Singh, N. Umezawa, P. Rinke, G. Kresse are gratefully acknowledged.

References

1. Jagadish, C., Pearton, S.J. (eds.): Zinc Oxide Bulk, Thin Films, and Nanostructures. Elsevier, New York (2006)
2. Look, D.C.: Recent advances in ZnO materials and devices. Mater. Sci. Eng. B **80**, 383 (2001)
3. Ozgür, Ü., Alivov, Y.I., Liu, C., Teke, A., Reshchikov, M.A., Dogan, S., Avrutin, V., Cho, S.-J., Morkoç, H.: A comprehensive review of ZnO materials and devices. J. Appl. Phys. **98**, 041301 (2005)
4. Janotti, A., Van de Walle, C.G.: Fundamentals of zinc oxide as a semiconductor. Rep. Prog. Phys. **72**, 126501 (2009)
5. McCluskey, M.D., Jokela, S.J.: Defects in ZnO. J. Appl. Phys. **106**, 071101 (2009)
6. Gordon, R.G.: Criteria for choosing transparent conductors. Mater. Res. Soc. Bull. **25**, 52 (2000)
7. Hosono, H.: Recent progress in transparent oxide semiconductors: Materials and device application. Thin Solid Films **515**, 6000 (2007)
8. Linsebigler, A.L., Lu, G., Yates Jr., J.T.: Photocatalysis on TiO_2 Surfaces: Principles, Mechanisms, and Selected Results. Chem. Rev. **95**, 735 (1995)
9. Kröger, F.A.: The Chemistry of Imperfect Crystals. North Holland Publishing, Amsterdam (1974)
10. Look, D.C., Hemsky, J.W., Sizelove, J.R.: Residual native shallow donor in ZnO. Phys. Rev. Lett. **82**, 2552–2555 (1999)
11. Tomlins, G.W., Routbort, J.L., Mason, T.O.: Zinc self-diffusion, electrical properties, and defect structure of undoped, single crystal zinc oxide. J. Appl. Phys. Rev. **87**, 117–123 (2000)
12. Dawar, A.L., Jain, A.K., Jagadish, C.: Semiconducting Transparent Thin Films. Institute of Physics, London (1995)
13. Nowotny, J., Radecka, M., Rekas, M., Sugihara, S., Vance, E.R., Weppner, W.: Electronic and ionic conductivity of TiO_2 single crystal within the n-p transition range. Ceram. Int. **24**, 571 (1998)
14. Diebold, U.: The surface science of titanium dioxide. Surf. Sci. Rep. **48**, 53 (2003)
15. Nowotny, M.K., Bak, T., Nowotny, J.: Electrical properties of single crystal TiO2. I. Electrical conductivity. J. Phys. Chem. B **110**, 16270 (2006)
16. Janotti, A., Van de Walle, C.G.: Oxygen vacancies in ZnO. Appl. Phys. Lett. **87**, 122102 (2005)
17. Janotti, A., Van de Walle, C.G.: New insights into the role of native point defects in ZnO. J. Cryst. Growth **287**, 58 (2006)

18. Janotti, A., Van de Walle, C.G.: Temperature dependence of Raman scattering in ZnO. Phys. Rev. B **75**, 165202 (2007)
19. Singh, A.K., Janotti, A., Scheffler, M., Van de Walle, C.G.: Sources of electrical conductivity in SnO_2. Phys. Rev. Lett. **101**, 055502 (2008)
20. Van de Walle, C.G.: Hydrogen as a cause of doping in zinc oxide. Phys. Rev. Lett. **85**, 1012 (2000)
21. Van de Walle, C.G., Neugebauer, J.: Universal alignment of hydrogen levels in semiconductors, insulators and solutions. Nature **423**, 626 (2003)
22. Van de Walle, C.G.: Hydrogen as a shallow center in semiconductors and oxides. Phys. Status Solidi B **235**, 89 (2003)
23. Janotti, A., Van de Walle, C.G.: Hydrogen multicentre bonds. Nat. Mater. **6**, 44 (2007)
24. Varley, J.B., Janotti, A., Singh, A.K., Van de Walle, C.G.: Hydrogen interactions with acceptor impurities in SnO_2: First-principles calculations. Phys. Rev. B **79**, 245206 (2009)
25. McCluskey, M.D., Jokela, S.J.: Sources of n-type conductivity in ZnO. Phys. B **401–402**, 355 (2007)
26. Lyons, J.L., Janotti, A., Van de Walle, C.G.: Role of Si and Ge as impurities in ZnO. Phys. Rev. B **80**, 205113 (2009)
27. Cox, S.F.J., Davis, E.A., Cottrell, S.P., King, P.J.C., Lord, J.S., Gil, J.M., Alberto, H.V., Vilão, R.C., Piroto Duarte, J., Ayres de Campos, N., Weidinger, A., Lichti, R.L., Irvine, S.J.C.: Experimental confirmation of the predicted shallow donor hydrogen state in zinc oxide. Phys. Rev. Lett. **86**, 2601 (2001)
28. Lavrov, E.V., Börrnert, F., Weber, J., Van de Walle, C.G., Helbig, R.: Hydrogen-related defects in ZnO studied by infrared absorption spectroscopy. Phys. Rev. B **66**, 165205 (2002)
29. Jokela, S.J., McCluskey, M.D.: Structure and stability of O-H donors in ZnO from high-pressure and infrared spectroscopy. Phys. Rev. B **72**, 113201 (2005)
30. Lavrov, E.V., Börrnert, F., Weber, J.: Dominant hydrogen-oxygen complex in hydrothermally grown ZnO. Phys. Rev. B **71**, 035205 (2005)
31. Alvin Shi, G., Stavola, M., Pearton, S.J., Thieme, M., Lavrov, E.V., Weber, J.: Hydrogen local modes and shallow donors in ZnO. Phys. Rev. B **72**, 195211 (2005)
32. Lavrov, E.V., Herklotz, F., Weber, J.: Identification of two hydrogen donors in ZnO. Phys. Rev. B **79**, 165210 (2009)
33. Hlaing Oo, W.M., Tabatabaei, S., McCluskey, M.D., Varley, J.B., Janotti, A., Van de Walle, C.G.: Calibrating dipolar interaction in an atomic condensate. Phys. Rev. B **82**, 193201 (2010)
34. Van de Walle, C.G., Laks, D.B., Neumark, G.F., Pantelides, S.T.: First-principles calculations of solubilities and doping limits: Li, Na, and N in ZnSe. Phys. Rev. B **47**, 9425 (1993)
35. Van de Walle, C.G., Neugebauer, J.: First-principle calculations for defects and impurities: Applications to III-nitrides. J. Appl. Phys. **95**, 3851 (2004)
36. Van de Walle, C.G., Lyons, J.L., Janotti, A.: Controlling the conductivity of InN. Phys. Status Solidi A **207**, 1024 (2010)
37. Dean, J.A.: Lange's Handbook of Chemistry, 14th edn. McGraw-Hill, New York (1992)
38. Hohenberg, P., Kohn, W.: Inhomogeneous electron gas. Phys. Rev. **136**, B864 (1964)
39. Kohn, W., Sham, L.J.: Self-consistent equations including exchange and correlation effects. Phys. Rev. **140**(4A), A1133–A1138 (1965)
40. Perdew, J.P., Wang, Y.: Liquid-drop model for crystalline metals: Vacancy-formation, cohesive, and face-dependent surface energies. Phys. Rev. Lett. **66**, 508 (1991)
41. Perdew, J.P., Burke, K., Ernzerhof, M.: Generalized gradient approximation made simple. Phys. Rev. Lett. **77**, 3865 (1996)
42. Anisimov, V.I., Aryasetiawan, F., Lichtenstein, A.I.: First-principles calculations of the electronic structure and spectra of strongly correlated systems: the LDA+U method. J. Phys. Condens. Matter **9**, 767 (1997)
43. Heyd, J., Scuseria, G.E., Ernzerhof, M.: Hybrid functionals based on a screened Coulomb potential. J. Chem. Phys. **118**, 8207 (2003)

44. Janotti, A., Varley, J.B., Rinke, P., Umezawa, N., Kresse, G., Van de Walle, C.G.: Hybrid functional studies of the oxygen vacancy in TiO2. Phys. Rev. B **81**, 085212 (2010)
45. Hedin, L.: New method for calculating the one-particle Green's function with application to the electron-gas problem. Phys. Rev. **139**, A796–A823 (1965)
46. Godby, R.W., Schlüter, M., Sham, L.J.: Accurate exchange-correlation potential for silicon and its discontinuity on addition of an electron. Phys. Rev. Lett. **56**, 2415–2418 (1986)
47. Rinke, P., Janotti, A., Scheffler, M., Van de Walle, C.G.: Defect formation energies without the band-gap problem: combining density-functional theory and the GW approach for the silicon self-interstitial. Phys. Rev. Lett. **102**, 026402 (2009)
48. Blöchl, P.E.: Projector augmented-wave method. Phys. Rev. B **50**, 17953 (1994)
49. Kresse, G., Joubert, D.: From ultrasoft psuedopotentials to the projector augmented-wave method. Phys. Rev. B **59**, 1758 (1999)
50. Kresse, G., Furthmüller, J.: Efficient iterative schemes for ab initio total-energy calculations using a plane-wave basis set. Phys. Rev. B **54**, 11169 (1996)
51. Kresse, G., Furthmüller, J.: Efficiency of ab-initio total energy calculations for metals and semiconductors using a plane-wave basis set. Comput. Mat. Sci. **6**, 15 (1996)
52. Wang, Z.L.: Zinc oxide nanostructures: growth, properties and applications. J. Phys. Condens. Matter **16**, R829–R858 (2004)
53. Look, D.C., Reynolds, D.C., Sizelove, J.R., Jones, R.L., Litton, C.W., Cantwell, G., Harsch, W.C.: Electrical properties of bulk ZnO. Solid State Commun. **105**, 399 (1998)
54. Look, D.C., Reynolds, D.C., Litton, C.W., Jones, R.L., Eason, D.B., Cantwell, G.: Characterization of homoepitaxial p-type ZnO grown by molecular beam epitaxy. Appl. Phys. Lett. **81**, 1830 (2002)
55. Minegishi, K., Koiwai, Y., Kikuchi, Y., Yano, K., Kasuga, M., Shimizu, A.: Growth of p-type zinc oxide films by chemical vapor deposition. Jpn. J. Appl. Phys. 2 **36**, L1453 (1997)
56. Ye, Z.-Z., Lu, J.-G., Chen, H.-H., Zhang, Y.-Z., Wang, L., Zhao, B.-H., Huang, J.-Y.: Preparation and characterization of p-type ZnO films by DC reactive magnetron sputtering. J. Cryst. Growth **253**, 258 (2003)
57. Kim, K.K., Kim, H.S., Hwang, D.K., Lim, J.H., Park, S.J.: Realization of p-type ZnO thin films via phosphorous doping and thermal activation of the dopant. Appl. Phys. Lett. **83**, 63 (2003)
58. Ryu, Y.R., Lee, T.S., White, H.W.: Properties of arsenic-doped p-type ZnO grown by hybrid beam deposition. Appl. Phys. Lett. **83**, 87 (2003)
59. Xiu, F.X., Yang, Z., Mandalapu, L.J., Zhao, D.T., Liu, J.L.: High-mobility Sb-doped p-type ZnO by molecular beam epitaxy. Appl. Phys. Lett. **87**, 152101 (2005)
60. Tsukazaki, A., Ohtomo, A., Onuma, T., Ohtani, M., Makino, T., Sumiya, M., Ohtani, K., Chichibu, S.F., Fuke, S., Segawa, Y., Ohno, H., Koinuma, H., Kawasaki, M.: Repeated temperature modulation epitaxy for p-type doping and light-emitting diode based on ZnO. Nat. Mater. **4**, 42 (2005)
61. Vlasenko, L.S., Watkins, G.D.: Optical detection of electron paramagnetic resonance in room-temperature electron-irradiated ZnO. Phys. Rev. B **71**, 125210 (2005)
62. Wang, X.J., Vlasenko, L.S., Pearton, S.J., Chen, W.M., Buyanova, I.A.: Oxygen and zinc vacancies in As-grown ZnO single crystals. J. Phys. D Appl. Phys. **42**, 175411 (2009)
63. Oba, F., Togo, A., Tanaka, I., Paier, J., Kresse, G.: Defects energetics in ZnO: A hybrid Hartee-Fock density functional study. Phys. Rev. B **77**, 245202 (2008)
64. Thomas, D.G., Lander, J.J.: Hydrogen as a donor in zinc oxide. J. Chem. Phys. **25**, 1136 (1956)
65. Wardle, M.G., Goss, J.P., Briddon, P.R.: First-principle study of the diffusion of hydrogen in ZnO. Phys. Rev. Lett. **96**, 205504 (2006)
66. Shi, G.A., Stavola, M., Pearton, S.J., Thieme, M., Lavrov, E.V., Weber, J.: Hydrogen local modes and shallow donors in ZnO. Phys. Rev. B **72**, 195211 (2005)
67. Myong, S.Y., Baik, S.J., Lee, C.H., Cho, W.Y., Lim, K.S.: Extremely transparent and conductive ZnO: Al thin films prepared by photo-assisted metalorganic chemical vapor deposition (photo-MOCVD) using $AlCl_3(6H_2O)$ as new doping material. Jpn. J. Appl. Phys. 2 **36**, L1078 (1997)

68. Ko, H.J., Chen, Y.F., Hong, S.K., Wenisch, H., Yao, T., Look, D.C.: Ga-doped ZnO films grown on GaN templates by plasma-assisted molecular-beam epitaxy. Appl. Phys. Lett. **77**, 3761 (2000)
69. Janotti, A., Snow, E., Van de Walle, C.G.: A pathway to p-type wide-band-gap semiconductors. Appl. Phys. Lett. **95**, 172109 (2009)
70. Kolmakov, A., Klenov, D.O., Lilach, Y., Stemmer, S., Moskovits, M.: Enhanced gas sensing by individual SnO_2 nanowires and nanobelts functionalized with Pd catalyst particles. Nano Lett. **5**, 667 (2005)
71. Baik, J., Zielke, M., Kim, M.H., Turner, K.L., Wodtke, A.M., Moskovits, M.: Tin-oxide-nanowire-based electronic nose using heterogeneous catalysis as a functionalization strategy. ACS Nano **4**, 3117 (2010)
72. Jarzebski, Z.M., Morton, J.P.: Physical properties of SnO_2 materials. J. Electrochem. Soc. **123**, 299C (1976)
73. Fonstad, C.G., Rediker, R.H.: Electrical properties of high-quality stannic oxide crystals. J. Appl. Phys. **42**, 2911 (1971)
74. Samson, S., Fonstad, C.G.: Defect structure and electronic donor levels in stannic oxide crystals. J. Appl. Phys. **44**, 4618 (1973)
75. Nagasawa, M., Shionoya, S.: Properties of oxidized SnO_2 single crystals. Jpn. J. Appl. Phys. **10**, 727 (1971)
76. Ohlsen, W.D., Johnson, O.W.: "Vacuum reduction" of rutile. J. App. Phys. **44**, 1927 (1973)

http://www.springer.com/978-1-4419-9930-6

Functional Metal Oxide Nanostructures
Wu, J.; Cao, J.; Han, W.-Q.; Janotti, A.; Kim, H.-C. (Eds.)
2012, XI, 368 p., Hardcover
ISBN: 978-1-4419-9930-6